LATENT HEATING FROM TRMM AND GPM MEASUREMENT

Wei-Kuo Tao[1], Steve Lang[2] and Taka Iguchi[3]

[1]NASA Goddard Space Flight Center, Greenbelt, MD 20771, USA, Wei-Kuo.Tao-1@nasa.gov

[2]*Science Systems and Applications, Inc.*

[3]Earth System Science Interdisciplinary Center, *University of Maryland*

ABSTRACT

The Goddard Convective-Stratiform Heating (CSH) algorithm, used to estimate cloud heating in support of the Tropical Rainfall Measuring Mission (TRMM), is upgraded in support of the Global Precipitation Measurement mission (GPM). The algorithm is required to use look-up-tables (LUTs) from cloud-resolving model (CRM) simulations from the Goddard Cumulus Ensemble model (GCE). This paper will present the heating retrievals from the Goddard CSH algorithm in the TRMM and GPM using precipitation products (rainfall, radar reflectivity).

Index Terms— Precipitation, Latent Heating, satellite

1. INTRODUCTION

Rainfall production is a fundamental process within the Earth's hydrological cycle because it represents both a principal forcing term in surface water budgets, and its energetics corollary, latent heating, is the principal source of atmospheric diabatic heating. Latent heat release itself is a consequence of phase changes between the vapor, liquid, and frozen states of water. The properties of the vertical distribution of latent heat release modulate large-scale meridional and zonal circulations within the Tropics - as well as modify the energetic efficiencies of mid-latitude weather systems. This paper highlights the retrieval of latent heat release from satellite measurements generated by the Tropical Rainfall Measuring Mission (TRMM) and Global Precipitation Mission (GPM) satellite observatory, which were launched in November 1997 and February 2014, respectively. Both TRMM and GPM measurements have been providing an accurate four-dimensional account of rainfall over the global Tropics and mid-latitudes: information that can be used to estimate the space-time structure of latent heating.

2. TRMM AND GPM LH ALGORITHMS

Two sets of latent heating retrieval algorithm methodologies (CSH, and Japan Spectral Latent Heating or SLH) have been developed to estimate latent heating based on rain rate profile retrievals obtained from TRMM and GPM measurements. Table 1 shows the differences between CSH and SLH algorithm in terms of their respective inputs and products. The table also provides the main references of their algorithms, including the developments, improvements and performances. Table 2 lists the required data and type of heating products for CSH algorithm. Note that one of the major inputs for the standard products is the improved rainfall estimate. Figure 1 shows an example of the LH products generated from the new version of the CSH algorithm (Lang and Tao, 2018).

	SLH	CSH
Key References	Shige *et al.* (2003, 2007,2008, 2009)	Tao *et al.* (1993; 2000; 2001, 2010), Lang *et al.* (2003); Lang and Tao (2018)
Cases	Tropics: COARE Winter: 6 events (all over oceans)	Tropics: 9 field campaigns (land and ocean) Winter: 6 events (land and ocean)
Inputs	PR/DPR	Combined
Products	LH, Q1R	Tropics: LH, Qr eddy Winter and high latitudes: LH
Convective-Stratiform separation	PR/DPR	GCE method (Tao *et al.* 2003)
Look-up Tables	No horizontal eddy Based on CRM (whole) domain and time averaged : Consistent with surface rainfall	Include horizontal and vertical eddy Subset (32 or 64 out of 512 whole domain)
19 vs 80 vertical layers	Reduced heating	Increase heating

Table 1 Summary of the five LH algorithms participating. Data inputs, retrieved products, and salient references included. Note the conventional relationship between Q_1 (apparent heat source), LH, and Q_R (radiative heating) is expressed by Q_1-Q_R = LH + EHT, where the final term represents eddy heat transport by clouds (noting that vertically

integrated EHT is zero, i.e., it provides no explicit influence on surface rainfall). Note that CSH and SLH explicitly use CRM-simulated latent heating profiles in their heating algorithm look up tables.

	Type	Spatial scale	Temporal scale	Retrieved Products
CSH-Combined	Gridded Orbital	0.25° x 0.25° 80 layers	Instantaneous	LH, EHT, Q_R, micro/eddy Q_2
CSH-Combined	Gridded Monthly	0.25° x 0.25° 80 layers	Monthly	LH, EHT, Q_R, micro/eddy Q_2
CSH-Combined	Orbital*	Pixel 80 layers	Instantaneous	LH, EHT, Q_R, micro/eddy Q_2

*Table 2 GPM cloud heating and moistening products from the CSH algorithm. The three individual heating components of the total apparent heat source or Q_1 (i.e., LH, EHT, and Q_R) retrieved separately where LH is latent heating, EHT the eddy heating rate, and Q_R the radiative heating/cooling rate. Likewise, the apparent moistening source or Q_2 is separated into its microphysical and eddy components. *Orbital (pixel) heating is available but not a standard GPM product. Note that the CSH will only have LH and QR outside TRMM region.*

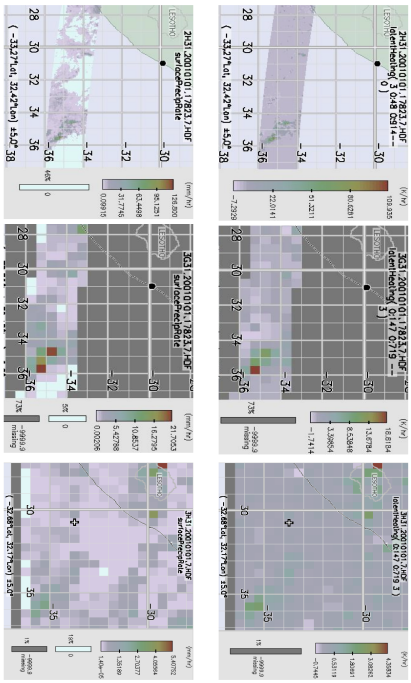

Fig. 1 LH products (left) from the version 2 CSH algorithm based on V7 rainfall data from the TRMM Combined Algorithm: (bottom) instantaneous pixel scale LH off the southeast coast of Africa 1 January 2001 at a height near 2.5 km from the orbital product, (middle) same but for the 3G31 gridded (0.5° x 0.5°) orbital product, and (top) same but for monthly mean LH from the 3H31 gridded monthly product.

3. RESULTS

Figure 2 shows the mean surface rainfall from the Combined algorithm for the 3-month period 1 April – 30 June 2014 for TRMM (i.e., 2B31, bottom panel) and for GPM (i.e., DPRGMI, top panel) over the TRMM domain (i.e., 37 N to 37 S). The rainfall is gridded onto a 0.5° x 0.5° grid for TRMM and a 0.25° x 0.25° grid from GPM, which are the official grid resolutions for TRMM and GPM gridded products, respectively, including gridded CSH heating products. Prominent rainfall features commonly observed within the Tropics in association with the ITCZ, the SPCZ, the Maritime Continent and midlatitude storm tracks over and downwind of the continents are all evident. In terms of the rainfall characteristics, the TRMM rainfall tends to have more moderate values (i.e., 4 to 6 mm/day, shown in green) whereas GPM shows large areas of higher values (i.e., > 10 mm/day). This is partially due to the increased averaging of the coarser TRMM grid, but also because GPM can detect more rain. The TRMM average surface rain rate over the entire domain and 3-month period is 2.8 mm/day, whereas for GPM, it is 3.3 mm/day

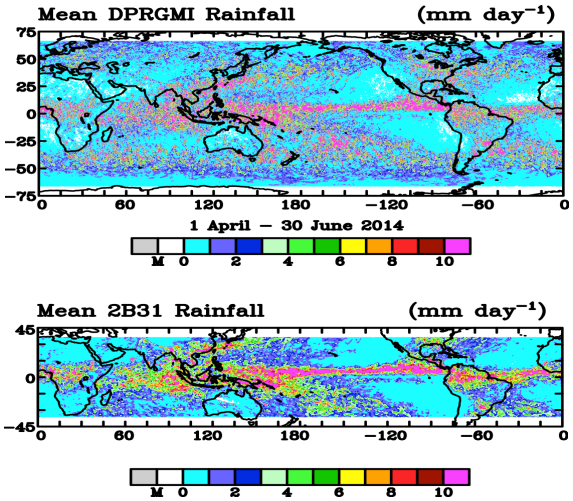

Fig. 2 Mean surface rainfall rates over the global Tropics (i.e., the TRMM domain) for the 3-month period 1 April to 30 June 2014 from the GPM Combined algorithm (DPRGMI, top panel) and the TRMM Combined algorithm (2B31, bottom panel).

Figures 3 and 4 show the mean diabatic heating rates ($Q_1 - Q_r$) over the TRMM domain during this same 3-month period retrieved from the CSH algorithm at 2 and 7 km, respectively. The lower panels show TRMM CSH-retrieved heating and the top panels show GPM CSH-retrieved heating using the new LUTs binned according to echo top height and low-level reflectivity gradient. Immediately evident is the large increase in shallow heating in both GPM retrievals over TRMM at low levels. At 2 km (Fig.

3), there is both much more intense heating within the hot spots already apparent in TRMM (e.g., the ITCZ, SPCZ, and equatorial Indian Ocean) as well as an intensification and expansion of shallow heating outside of these regions into the sub-tropics. This is tied to the increased detection of shallow, mostly convective rain. Both the composite and the split echo top versions of the new LUTs show similar robust heating patterns at the 2-km level. At upper-levels (Fig. 4), the heating patterns and mean intensities are fairly similar between the GPM and TRMM retrievals with strong areas of heating over equatorial Africa, northern South America, the Maritime Continent, and within a sharp, well-defined ITCZ extending across the Central and East Pacific. Other areas of prominent heating in the equatorial Atlantic, the SPCZ, and the equatorial Indian Ocean are also similar in shape and magnitude when accounting for the coarser TRMM grid resolution.

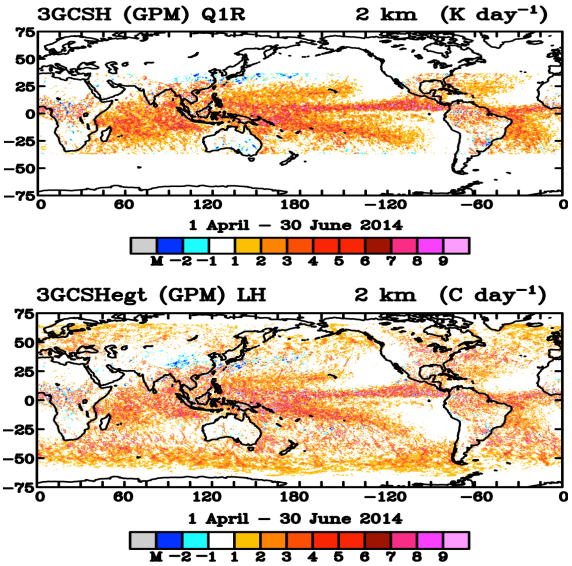

Fig. 3 Mean diabatic heating rates ($Q_1 - Q_r$) at 2 km AGL for the 3-month period 1 April to 30 June 2014 retrieved from the CSH algorithm using rainfall data from the Combined algorithm for GPM with new CSH LUTs differentiated by echo top height and low-level (0-2 km) reflectivity gradient (top panel) and from TRMM with the current V7 CSH LUTs (bottom panel).

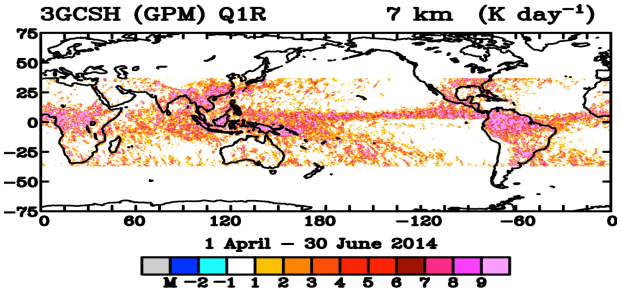

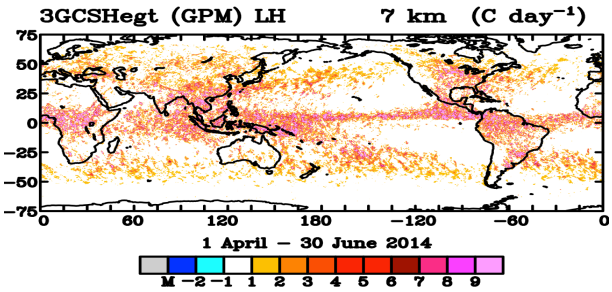

Fig. 4 Same as the Fig. 3 except for the 7-km level.

The retrieved heating can be vertically integrated to produce an equivalent surface rain rate, which can then be compared against the observed (input) surface rain rate to check for biases (Lang and Tao, 2018). Figure 5 shows the net difference in integrated heating minus the observed (input) surface rain rate from the Combined algorithm over the global. A consistent pattern emerges for the retrieval with broad areas of surplus heating occurring over ocean in the weaker rain rate regimes poleward of the ITCZ and heating deficits occurring primarily over ocean at even higher latitudes along the edges of the midlatitude storm tracks. These areas are dominated by convective and stratiform rain, respectively, which is consistent with the imbalance in heating versus rainfall for these two regions in convective systems as some of the condensate generated in the convective region, which produces heating there, falls out as precipitation in the stratiform region. deficit heating such as within the ITCZ, equatorial Africa, and tropical South America. The zonal mean differences is less than 0.5 mm d-1. Also integrated heating is always stronger than observed in all latitudes and smaller differences is in sub-tropics.

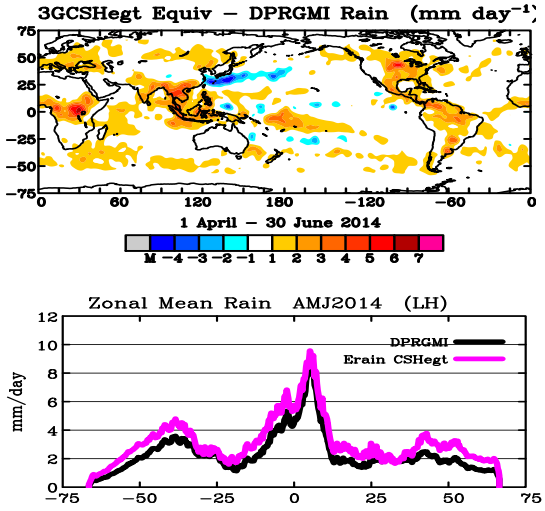

Fig. 5 (Top) Mean retrieved heating rate bias obtained by differencing the mean surface rainfall rate from the Combined algorithm from the mean

column-integrated less CSH cloud diabatic heating rates ($Q_1 - Q_r$) for the 3-month period 1 April to 30 June 2014 for GPM with new CSH algorithm. Bottom panel is the zonal mean retrieval and GPM combined rain.

4. CURRENT WORKS

Additional model grid configurations (3D, quasi-3D), domain sizes (1024 or more) and resolutions (200 m – smaller, shallower clouds) for LUTs will be tested. Winter and high latitudes cases (for both oceanic and continental region) is currently adding into LCTs (Tao *et al.* 2018). In addition, validation (integrated heating vs rainfall at higher latitudes, model self- consistency tests) will be studied. Both CSH and SLH teams are working closely in terms of sharing GCE, WRF and JMA model simulated latent heating structures (improving the look-up tables). The microphysical processes (or schemes) used in the GCE and WRF model are being improved by using GMP ground validation (GV) data sets.

REFERENCES

Lang, S., W.-K. Tao, R. Cifelli, W. Olson, J. Halverson, S. Rutledge, and J. Simpson, 2007: Improving simulations of convective system from TRMM LBA: Easterly and Westerly regimes. *J. Atmos. Sci.,* **64**, 1141-1164.

Lang, E. S., and W.-K. Tao, 2018: The Next-generation Goddard Convective-Stratiform Heating Algorithm: New Tropical and Warm Season Retrievals for GPM. *J. Climate*, (in press).

Shige, S., Y. N. Takayabu, W.-K. Tao and D. Johnson, 2003: Spectral retrieved of latent heating profiles from TRMM PR data. Part I: Algorithm development with a cloud resolving model. *J. Applied Meteor.* **43**, 1095-1113.

Shige, S., Y. N. Takayabu, W.-K. Tao and D. E. Johnson, 2004: Spectral retrieval of latent heating profiles from TRMM PR data. Part I: Development of a model-based algorithm. *J. Applied Meteor.,* **43**, 1095-1113.

Shige, S., Y. N. Takayabu, W.-K. Tao and C.-L. Shie, 2007: Spectral retrieval of latent heating profiles from TRMM PR data. Part II: Algorithm improvement and heating estimates over tropical ocean regions. *J. Applied Meteor.,* **46**, 1098-1124.

Shige, S., Y. N. Takayabu, and W.-K. Tao, 2008: Spectral retrieval of latent heating profiles from TRMM PR data. Part III: Estimating apparent moisture sink profiles over tropical oceans. *J. Applied Meteor. Climatol.,* **47**, 620-640.

Shige, S., Y. N. Takayabu, S. Kida, W.-K. Tao, X. Zeng and T. L'Ecuyer, 2009: Spectral retrieved of latent heating profiles from TRMM PR data. Part VI: Comparisons of lookup tables from two- and three-dimensional simulations. *J. Climate,* **22**, 5577-5594.

Takayabu, Y. N., S. Shige, W.-K. Tao and N. Hirota, 2010: Shallow and deep latent heating modes over tropical oceans observed with TRMM PR spectral latent heating data. *J. Climate,* **23,** 2030-2046.Tao, W.-K., S. Lang, J. Simpson, and R. Adler, 1993: Retrieval algorithms for estimating the vertical profiles of latent heat release: Their applications for TRMM. *J. Meteor. Soc. Japan*, **71**, 685-700.

Tao, W.-K., J. Simpson, S. Lang, M. McCumber, R. Adler and R. Penc, 1990: An algorithm to estimate the heating budget from vertical hydrometeor profiles. *J. Appl. Meteor.,* **29**, 1232-1244.

Tao, W.-K., S. Lang, J. Simpson, W.S. Olson, D. Johnson, B. Ferrier, C. Kummerow, and R. Adler, 2000: Retrieving vertical profiles of latent heat release in TOGA COARE convective systems using a cloud resolving model, SSM/I and radar data. *J. Meteor. Soc. Japan,* **78**, 333-355.

Tao, W.-K., S. Lang, W.S. Olson, S. Yang, R. Meneghini, J. Simpson, C. Kummerow, E. Smith and J. Halverson, 2001: Retrieved vertical profiles of latent heating release using TRMM rainfall products for February 1998. *J. Appl. Meteor.,* **40**, 957-982.

Tao, W.-K., E.A. Smith, R.F. Adler, Z.S. Haddad, A.Y. Hou, T. Iguchi, R. Kakar, T.N. Krishnamurti, C.D. Kummerow, S. Lang, R. Meneghini, K. Nakamura, T. Nakazawa, K. Okamoto, W.S. Olson, S. Satoh, S. Shige, J. Simpson, Y. Takayabu, G.J. Tripoli, and S. Yang, 2006: Retrieval of latent heating from TRMM measurements. *Bull. Amer. Meteor. Soc.,* **87,** 1555-1572.

Tao, W.-K., S. Lang, X. Zeng, S. Shige, and Y. Takayabu, 2010: Relating convective and stratiform rain to latent heating. *J. Climate*, **23**, 1874–1893.

Tao, W.-K., Y. N. Takayabu, S. Lang, S. Shige, W. Olson, A. Hou, G. Skofronick-Jackson, X. Jiang, C. Zhang, W. Lau, T. Krishnamurti, D. Waliser, M. Grecu, P. E. Ciesielski, R. H. Johnson, R. Houze, R. Kakar, K. Nakamura, S. Braun, S. Hagos, R. Oki and A. Bhardwaj, 2016a: TRMM Latent Heating Retrieval: Applications and Comparisons with Field Campaigns and Large-Scale Analyses, *AMS Meteorological Monographs - Multi-scale Convection-Coupled Systems in the Tropics,* **56,** Chapter 2, 2.1-2.34.

Tao, W.-K., S. Lang, and T. Iguchi, 2018: Goddard latent heating algorithm for GPM, *J. Climate* (to be submitted).